



Hydrogen production from pruning waste biomass by integration of hydrothermal treatment and aqueous phase reforming

M. Torres, J. Justicia, J.A. Baeza, L. Calvo, F. Heras^{*}, M.A. Gilarranz

Department of Chemical Engineering, Universidad Autónoma de Madrid, Ciudad Universitaria de Cantoblanco, 28049, Madrid, Spain

ARTICLE INFO

Handling Editor: Dr M Mahdi Najafpour

Keywords:

Waste biomass
Hydrogen
Aqueous phase reforming
Pt/C catalyst

ABSTRACT

This research investigates hydrogen production from urban pruning waste biomass through combined hydrothermal treatment and aqueous phase reforming. Optimization of treatment parameters (temperature, time and pH) yielded a hydrolysate rich in water-soluble compounds. The most effective conditions were found at 180 °C and 60 min, achieving a balanced hydrolysis and solubilization of lignocellulosic waste. Low pH, induced by organic acids from the waste, drove hydrotreatment, but further acid addition hindered solubilization. Aqueous phase reforming at 220 °C with a carbon-supported Pt catalyst resulted in enhanced carbon conversion and H₂ production at an initial carbon concentration of 1,000 mg/L. Increasing Pt load from 3 to 5 % wt. improved production and selectivity, plateauing at 7.5 % wt. Optimal conditions demonstrated a H₂ production of 17 mmol per gram of dissolved organic carbon, affirming the viability of this scheme for pruning waste valorization.

1. Introduction

To limit the global warming, the United Nations Intergovernmental Panel on Climate Change called for a 25 % reduction in carbon emissions by 2070 compared to 2010 [1]. In this context, H₂ is an energy carrier with a major role in circular and sustainable economy contributing to decarbonization and thus to the reduction of greenhouse gas emissions [2,3]. Current H₂ production is equivalent to 4 % of the world energy consumption, therefore a dramatic increase in production is needed to achieve the proposed target in decarbonization [4]. Most of the produced H₂ is consumed in ammonia production (40 %), oil refining (37 %), methanol production (10 %) and other industries such as pharmaceutical, food and hydrogen peroxide production. The interest in H₂ as a renewable energy source is growing due to its potential as an environmentally friendly option. The European Union has selected H₂ as the key element for a sustainable development and energy model transition, setting ambitious targets for renewable H₂ production. The strategy aims to produce one million tons of renewable H₂ by 2024 and ten million tons by 2030 (EU Hydrogen Strategy), with the objective of using it in sectors that are difficult to decarbonize, such as heavy transport. H₂ will also be used for storage, as a backup function, improving security of supply in the medium term [5].

Nowadays, 95 % of global H₂ is produced from natural gas by Steam Methane Reforming process (SMR) [6], in which natural gas reacts with

steam in the presence of a catalyst, usually Ni supported on alumina, to generate syngas, composed of H₂ and CO₂ [7]. The process achieves conversions of around 80 % operating at severe conditions in the 700–1,000 °C and 3–25 bar ranges [8,9]. H₂ produced by SMR is non-renewable and is therefore currently outside the EU objective. An alternative commercial option for H₂ production is the electrolysis of water. This process uses electrical energy to break down the water molecule into hydrogen and oxygen. This a simple process which has as main advantage that renewable energy sources can be used for electricity supply [10], but the process efficiency is low, compromising competitiveness [11,12]. Photo-electrolysis is a technique that uses solar radiation and electrical energy for the same purpose as traditional electrolysis. Solar radiation is transformed into chemical energy through a semiconductor that absorbs the photons and splits water molecules. The main advantages of this technology are the potential use of renewable energy to obtain green H₂ and the absence of direct carbon emissions, while the main drawbacks currently are high costs and low efficiency [13].

The aqueous phase catalytic reforming (APR) process is based on the decomposition of oxygenated hydrocarbons in water liquid medium into H₂ and carbon oxides [14]. Light alkanes are also produced by secondary reactions [14]. The process typically operates at 210–270 °C and 10–50 bar [15], which can be considered as mild conditions compared to those used in conventional steam reforming, resulting in lower operating

^{*} Corresponding author.

E-mail address: fran.heras@uam.es (F. Heras).

<https://doi.org/10.1016/j.ijhydene.2024.03.182>

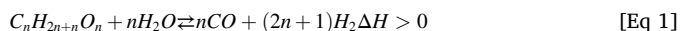
Received 26 January 2024; Received in revised form 4 March 2024; Accepted 13 March 2024

Available online 18 March 2024

0360-3199/© 2024 The Author(s). Published by Elsevier Ltd on behalf of Hydrogen Energy Publications LLC. This is an open access article under the CC BY-NC-ND license (<http://creativecommons.org/licenses/by-nc-nd/4.0/>).

costs.

The main reactions that take place in the APR process are reforming [Eq. (1)] and water-gas shift (WGS, [Eq. 2]). The last one is favored in the APR medium, whereby the gas stream is produced with very low CO content, which is an important advantage for subsequent H₂ separation and recovery since the presence of CO can limit their use in applications such as fuel cells [16].



The most used catalysts are based on noble metals such as Pt, Pd, Ru and Rh [17], but Pt catalysts showed particularly high selectivity towards H₂ due to their high activity in C–C bond cleavage [18].

The APR process can be carried out using different compounds and streams as feedstock [19]. Some of the compounds more studied as feedstocks are sugars, alcohols and organic acids [20–22], although biomasses and waste biomasses from food industry [23,24] and biorefinery schemes [25] are receiving increased attention since the produced H₂ can be considered as bio-H₂. Wastewater from several food industries has been studied as a substrate for APR, such as those based on starch from rice, potato, sweet potato and cassava [26], breweries [27, 28], tuna canneries [29], cheese production [30] or juice extraction [31]. Likewise, waste streams from bio-oil production at biorefineries can also be used as feedstock to APR for H₂ production [32]. In all these cases, the solubility in water of the feedstocks facilitates APR since reactions take place strictly in the liquid phase.

Particularly interesting is the solid waste biomass valorization by APR, which needs the integration of a prior stage to generate a water-soluble fraction for further processing. With this focus, maintaining both a high organic matter content and a composition favorable to APR in the HTC process water becomes pivotal [33]. This approach holds particular promise for sludges and other waste biomass with high moisture content, as alternative valorization methods would entail extremely expensive drying processes. A notable example involves the valorization of sewage sludge through the integration of hydrothermal carbonization (HTC) followed by APR of the process water produced. This approach has also been applied to the valorization of corn stover, and lignin-rich biomass fractions [33,34]. The solubilization of organic matter in the pretreatment results from the autohydrolysis of lignocellulosic components, driven by temperature and the acidic medium resulting from acetic acid released by the hydrolysis of acetate groups, primarily from hemicelluloses in the early stages of the pretreatment [35]. Autohydrolysis of lignocellulosic biomass typically yields a hydrolysate containing oligosaccharides, sugars, lignan, and lignin derivatives from the starting raw material [36]. Similarly, hydrothermal liquefaction has been reported as a preceding stage of APR, particularly in the case of lignocellulosic biomass [34,37]. Temperatures around 350 °C become essential to maximize the production of the liquid fraction, as solubilizing lignocellulosic biomass components proves challenging due to the crosslinked nature of the biopolymers composing it [38]. Hydrothermal treatments at lower temperatures (160–350 °C) are strategically employed to maximize the yield of water-insoluble solid products, which, as observed in the case of hydrochar, can be further valorized [39,40].

The current work explores the use of lignocellulosic pruning waste as feedstock to produce bio-H₂ by combination of hydrothermal treatment and APR. Pruning waste is a representative lignocellulosic biomass waste usually subjected to composting to produce low grade products, with few alternatives for valorization. Hydrothermal treatment is carried out in a wide range of conditions to study the behavior of the water-soluble fractions in APR, which is performed at different conditions for better integration of the bio-H₂ production.

2. Experimental procedure

2.1. Materials

The starting material used as feedstock for the valorization process was waste lignocellulosic biomass from urban pruning provided by the Madrid City Council, used as material for round robin test in the framework of BIO3 research project [41]. The biomass had a moisture of 5.23 %, as determined by drying at 105 °C for 3 h following the ISO 18134-0.3:2015 standard [42]. Ash content of 4.43 % was determined by calcination at 550 °C according to ISO 18122:2022 [43] standard. In addition, the biomass had a nitrogen content of 97 mg/kg and a COD of 1.241 gO₂/kg [44]. The composition in cellulose, hemicellulose and lignin was 45–53 %, 15–35 % and 25–29 %, respectively, as reported in a previous work [45].

Hexachloroplatinic acid solution (8 % wt. in water) purchased from Sigma Aldrich was used as precursor salt in the preparation of catalysts, and ENSACO250 carbon black (CB), supplied by Timcal Canada Inc. (Canada) was used as catalyst support. KOH (90 %, Panreac), HCl (37 %, Scharlau) and H₂SO₄ (97 %, Scharlau) were used to adjust pH of the reaction medium.

2.2. Synthesis and characterization of the catalyst

Pt supported in carbon black (CB) ENSACO250 was used as catalyst for APR runs. The Pt/CB catalysts were prepared with Pt nominal loads of 3, 5 and 7.5 % wt. using the incipient wetness impregnation procedure. The support was firstly impregnated with an aqueous solution of hexachloroplatinic acid and dried overnight at 60 °C. Later, the samples were calcined at 200 °C for 2 h and finally reduced under H₂ flow at 300 °C for 2 h. The CB support used was chosen due to the high hydrothermal stability that it exhibits under APR conditions thanks to its ordered structure [46]. In addition, the support has a low BET surface area of 65 m²/g [25], which avoids the accumulation of coke on the catalyst surface and, therefore, the deactivation of the catalyst by plugging of the active centres. The Pt content range was selected according to previous works on the APR of wastewater containing biomass-derived pollutants [23,47].

The prepared catalysts were textural characterized by N₂ adsorption/desorption isotherms at 77 K using a Micromeritics Tristar II device. The dispersion of the metal phase in the catalysts was analyzed by Transmission Electron Microscopy (TEM) with a JEOL JEM1400 microscope. ImageJ software was used to measure the size of Pt nanoparticles on TEM images. Fresh and used catalysts were also characterized by TPD/TPO using a TA Instruments Q500 equipment. To obtain the TPD curve, the sample was heated from room temperature to 900 °C with a heating ramp of 10 °C/min under a N₂ flow of 50 mL/min, then the samples were allowed to cool down to 100 °C. Subsequently TPO curve was obtained heating the sample to 900 °C with a heating ramp of 5 °C/min under 50 mL/min air flowrate. The relative abundance of Pt²⁺ and Pt⁰ species in the catalysts was determined after deconvolution of the Pt XPS spectrum, fitting the data by least squares to the Gaussian fit. Pt is located in the 4f_{7/2} and 4f_{5/2} orbitals. The Pt²⁺ species has a binding energy of 72.29 and 75.54 eV, respectively, while the Pt⁰ species has a binding energy of 71.13 and 74.45 eV, respectively. The spectrometer used for the analysis is a PHI 5000 VersaProbe II apparatus equipped with a 1486.6 eV X-Ray source at 25.1 W with a beam diameter of 100 µm.

2.3. Experimental procedure

Both the pretreatment of the starting biomass and APR experiments were carried out in 50 mL stainless steel pressure reactors (Berhof BR-100) with a Teflon liner, magnetic stirring (750 rpm) and temperature control provided by a hotplate stirrer (Heidolph - MR Hei-Standard). The reactors were inserted in an insulating and heating block that provides a heating ramp of 10 °C/h. Before each test, air was purged from the

Table 1

Textural properties for prepared catalyst with 3, 5 and 7.5 % wt. Pt load.

Pt load (% wt.)	S_{BET} (m^2/g)	A_{ext} (m^2/g)	Micropore Volume (cm^3/g)	Mesopore Volume (cm^3/g)
3	58	54	0.002	0.048
5	60	54	0.003	0.047
7.5	63	57	0.003	0.045

reaction system and the initial pressure was set at 3 and 5 bar for biomass pretreatment and APR, respectively, using argon.

The pretreatment of biomass consisted in a hydrothermal treatment focused to the hydrolysis and solubilization of the organic matter as hydrolysate. A volume of 15 mL of water was introduced into the reactor together with the precise biomass amount to achieve a water to dry solid fraction ratio of 10 to 1 (wt.) during pretreatment. Since the biomass

moisture content was previously determined as 5.23%, 1.58 g of raw biomass and 14.92 mL of water were placed into the reactor vessel.

The effect of the intensity of hydrolysis, 15 mL of hydrolysate, water diluted to achieve 1,000, 2,000 and 3,000 mgTOC/L, were placed in the reactor together with different catalyst loads (75–300 mg). The reactions were performed at 220 °C for 4 h,

For both pretreatment and APR runs, air in the reactor was initially purged with argon and an initial pressure of 3 bar is set. Pressure developed during the tests corresponded to combination of pressure at liquid-vapor equilibrium at operating temperature and initial pressure, thus 12–26 bar.

The gas phase produced in both pretreatment and APR experiments was collected in multilayer foil sample gas bags (Supelco, USA) and analyzed by Gas Chromatography on a GC/FID/TCD device (7820 A, Agilent). The Total Organic Carbon (TOC) concentration in the

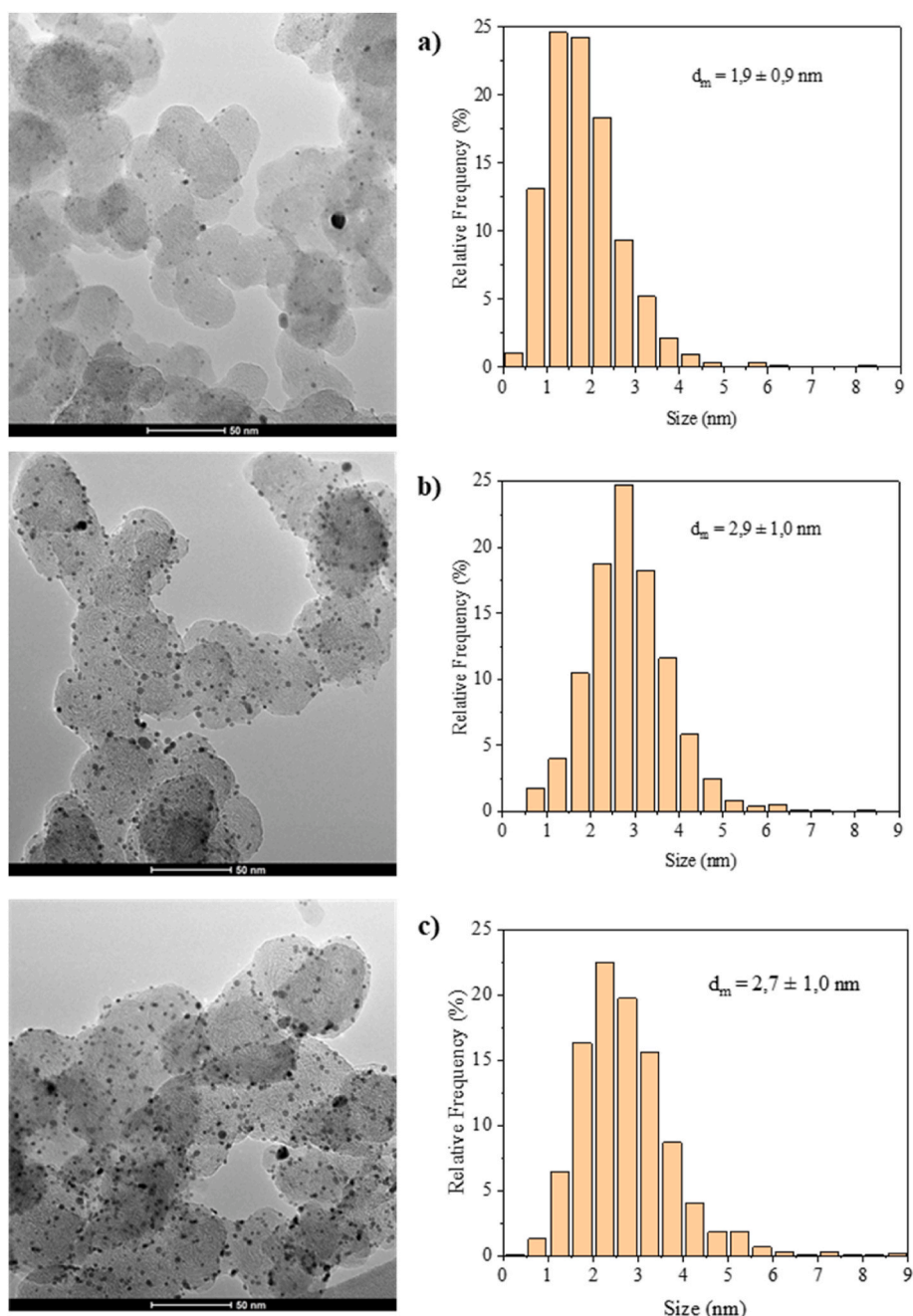


Fig. 1. TEM images and Pt particle size distribution of the fresh catalysts. a) 3 % Pt, b) 5 % Pt, c) 7.5 % Pt.

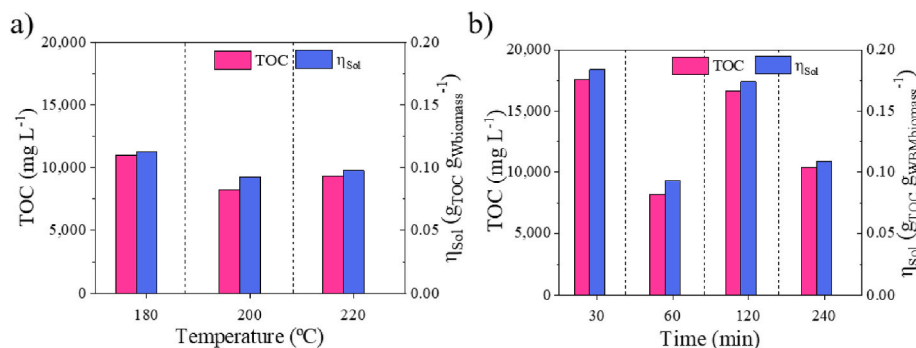


Fig. 2. TOC concentration in hydrolysate and solubilization yield in the pre-treatment of starting biomass at a) different temperatures (60 min), and b) different time (200 °C).

hydrolysate and in the APR effluent was determined with a TOC-VCSH (Shimadzu) equipment. Elemental Analysis of the starting biomass and solid phase resulting from the pretreatment was performed with a LECO CHNS-932 elemental analyzer.

The organic carbon solubilization yield during the pretreatment was calculated from TOC in the hydrolysate as shown in [Eq. (3)],

$$\eta_{sol} \left(\frac{\text{mg TOC}}{\text{mg biomass}} \right) = \frac{TOC \left(\frac{\text{mg}}{\text{L}} \right) \cdot V_{process\ water} (L)}{W_{biomass} (mg)} \quad [\text{Eq. 3}]$$

where $W_{biomass}$ is the weight of dry ash-free biomass used in the experiments.

In the APR reactions, TOC conversion and C conversion to gas products (CCgas) were calculated as shown by [Eqs. (4) and (5)], respectively. H_2 production was evaluated based on initial TOC fed to APR [Eq. (6)] and dry ash-free biomass [Eq. (7)]. Selectivity to H_2 was determined as a percent of the total gas production [Eq. (8)].

$$X_{TOC} (\%) = \frac{TOC_{initial} \left(\frac{\text{mg}}{\text{L}} \right) - TOC_{final} \left(\frac{\text{mg}}{\text{L}} \right)}{TOC_{initial} \left(\frac{\text{mg}}{\text{L}} \right)} \cdot 100 \quad [\text{Eq. 4}]$$

$$CC_{gas} (\%) = \frac{C_{gas} (g)}{TOC_{initial} \left(\frac{\text{g}}{\text{L}} \right) \cdot V_{liquid} (L)} \cdot 100 \quad [\text{Eq. 5}]$$

$$P_{H_2} \left(\frac{\text{mmol } H_2}{\text{g TOC}_{initial}} \right) = \frac{H_{2,produced} (\text{mmol})}{TOC_{initial} \left(\frac{\text{g}}{\text{L}} \right) \cdot V_{liquid} (L)} \quad [\text{Eq. 6}]$$

$$P_{H_2} \left(\frac{\text{mmol } H_2}{\text{g biomass}} \right) = P_{H_2} \left(\frac{\text{mmol } H_2}{\text{g TOC}_{initial}} \right) \cdot \eta_{sol} \left(\frac{\text{g TOC}}{\text{g biomass}} \right) \quad [\text{Eq. 7}]$$

$$S_{H_2} (\%) = \frac{H_{2,produced} (\text{mmol})}{\sum \text{gas produced} (\text{mmol})} \cdot 100 \quad [\text{Eq. 8}]$$

3. Results and discussion

3.1. Characterization of catalysts

The results of textural characterization are summarized in Table 1. As can be observed, the catalysts showed the textural properties corresponding to those of a material with such low porosity as the carbon black used as a support. i.e., S_{BET} almost negligible and similar to A_{ext} , not significant microporosity and moderate mesoporosity. In addition, these properties were not affected by the increase of Pt load.

The TEM images in Fig. 1 indicate that all the fresh catalysts showed a well dispersed Pt phase with very low prevalence of oversized nanoparticles and agglomerates. A slightly smaller mean nanoparticle size of ca. 1.9 nm can be observed for the 3 % wt. Pt catalyst. A similar mean size of 2.7–2.9 nm was obtained for the 5 and 7.5 % wt. Pt catalysts,

although both showed a high contribution of nanoparticles with size smaller than 2 nm.

Figure S1 (supplementary material) shows the thermogravimetric analysis of the fresh catalysts. In the TPD curves, a very slight mass loss is observed for the three catalysts with different Pt contents, indicating that they are very stable catalysts in inert atmosphere. In the TPO curves, significant mass loss is observed at temperatures between 400 and 500 °C. This weight loss is very similar for all catalysts and is attributed to the burn-off of the catalyst support.

XPS analyses of fresh Pt/CB catalysts with different Pt contents (see Fig. S2, supplementary material) showed that catalyst with 3 % wt. Pt has a Pt^{2+}/Pt^0 ratio of 0.61, which increases to 1.90 for the 5 % wt. Pt sample. The highest contribution of Pt species shifts from $4f_{5/2}$ to $4f_{7/2}$ orbital as the Pt content increases.

3.2. Solubilization of organic matter by biomass pretreatment

The lignocellulosic biomass was pretreated to produce a hydrolysate rich in organic matter suitable for APR stage, since APR reactions take place strictly in the liquid phase. Fig. 2a shows that TOC concentration in the hydrolysate was higher when biomass pretreatment was carried out at 180 °C. In these conditions, organic matter in the hydrolysate results mainly from hydrolysis of hemicellulose and, in lower extent, from solubilization and degradation of extractives and lignin; likewise, oligomers are hydrolyzed in higher extent to sugars as the temperature and time of the pretreatment is increased [48,49]. However, the increase of pretreatment temperature to 200 and 220 °C led to lower concentration of organic matter in the hydrolysate. This trend can be related to recondensation of lignin derivatives and other dissolved compounds at high temperature [48,50]. Thus, it was found that long autohydrolysis time at low temperature leads to higher condensation and lower content of lignin derivatives in the hydrolysate in comparison to when shorter time at high temperature were used; in addition, high temperature promotes dehydration of sugars and furfural formation [51]. Polysaccharides were also found to have a role in pseudo-lignin formation during acid hydrolysis [52]. Furthermore, as the pretreatment was carried out in batch mode, some precipitation of dissolved organic matter can be expected to take place upon reaction system cooling [53]. On the other hand, for the purpose of the current work, the biomass pretreatment was conducted in the 180–220 °C range to promote degradation of oligomers to sugars, although at these conditions HTC reactions are likely to occur, specially at the highest temperatures [54]. In previous works using the same biomass material, it was found that the yield to hydrochar for pretreatment for 1 h at 180 °C decreased from ca. 88 % to 74 and 68 % when temperature was increased to 210 and 230 °C, respectively [55]. Likewise, an enrichment in hydrochar carbon content took place, which is usually due to the formation of secondary hydrochar, involving degradation of dissolved carbon compounds and evolution of gases, contributing to lower TOC concentration in the

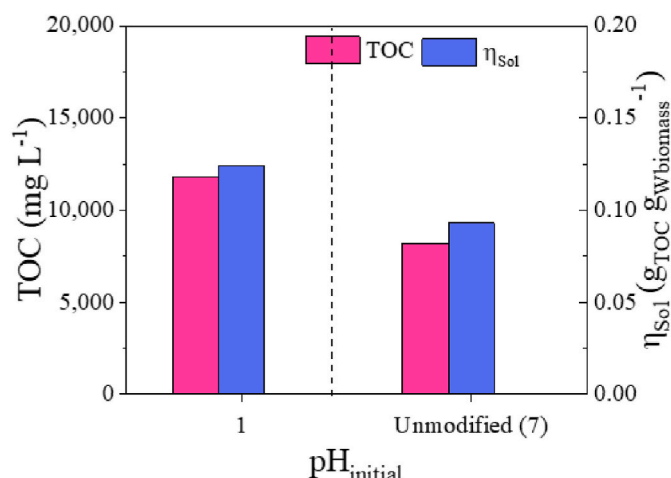


Fig. 3. TOC concentration in hydrolysate and solubilization yield in the pretreatment of starting biomass at different pH (60 min, 200 °C).

hydrolysate [56]. This can be evidenced with the decrease in volatile solids content previously observed for this biomass when the pretreatment temperature was increased from 180 to 230 °C [55]. Likewise, a higher release of high-molecular-weight and aromatic compounds into the hydrolysate was found at high temperature.

A relevant influence of pretreatment time in TOC concentration in the hydrolysate can be also observed in Fig. 2b, exhibiting a peak value of 18,000 mg/L at 30 min and declining at 60 min due to condensation and repolymerization reactions. Thus, it was observed that combination of time and temperature leads to condensation of solubilized components, particularly those derived from lignin [50,57]. Further increase in pre-treatment time led again to an increase in the concentration of organic matter, which can be associated mostly to additional hydrolysis

of hemicellulose fraction under the acidic medium developed in the autohydrolysis medium [58]. It has also to be noted that the combination of time and temperature leads to loss of oligomers and sugars from the hydrolysate [59,60] and formation of furfural, 5-hydroxymethylfurfural, organic acids and furanic compounds [36]. The further decline in TOC concentration at long pretreatment time can be ascribed to higher contribution of HTC reactions [61]. Again, formation of secondary hydrochar can be expected in some extent for the longest pretreatment time, which would justify the decrease in TOC concentration and would also involve intramolecular condensation, dehydration and decarboxylation of furanic and phenolic species derived from sugars and lignin derivatives, respectively [62].

Most of the reactions indicated above are driven by low pH developed in the pretreatment medium due to organic acid release. The effect of additional acidity in the starting medium can be observed in Fig. 3. When a starting pH value of 1 was used in the pretreatment, the TOC concentration in the hydrolysate increased by ca. 50 %. This increase is related to higher acid-driven hydrolysis of hemicellulose and cellulosic fractions [63]. In addition to higher TOC concentration, substantial changes can be expected in the composition of hydrolysate as dehydration or sugars and alcohols is boosted [64]. Breakage of lignin linkages is also promoted by acid medium, although also condensation and repolymerization are promoted when inorganic strong acids are used in hydrolysis [65,66].

3.3. APR of hydrolysate

The APR experiments showed that hydrolysate can be reformed with non-detectable generation of CO, indicating that WGS reaction is highly favored at all the reaction conditions tested. The concentration of organic matter in the starting reaction medium showed significant influence on the conversion achieved. Fig. 4 indicates that around 60 % of the starting organic carbon was converted in the experiments carried out with an initial concentration of 1,000 mg/L, decreasing below 40 %

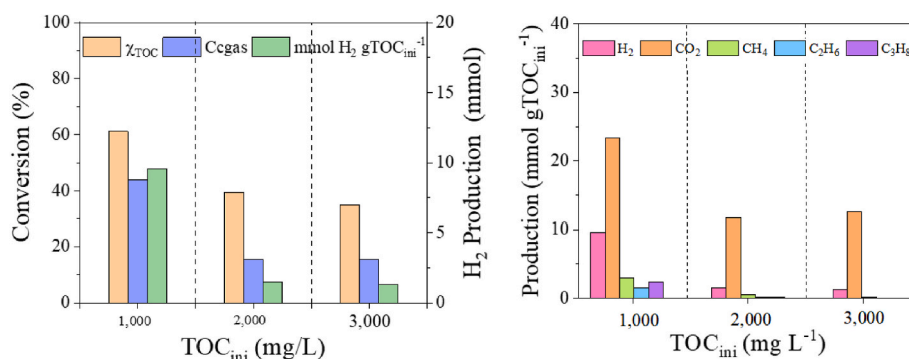


Fig. 4. APR of hydrolysate with different initial TOC concentration (pretreatment: 60 min, 180 °C; APR: 3 % wt. Pt/CB catalyst).

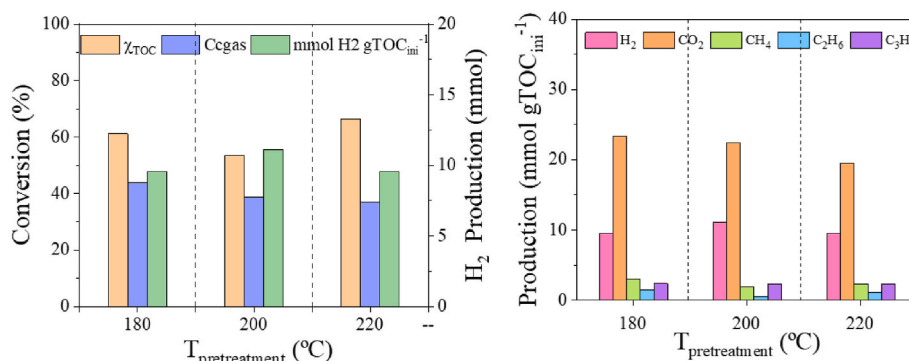


Fig. 5. APR of hydrolysate obtained at different temperatures (pretreatment: 60 min; APR: TOC_{ini} = 1,000 mg/L, 3 % wt. Pt/CB).

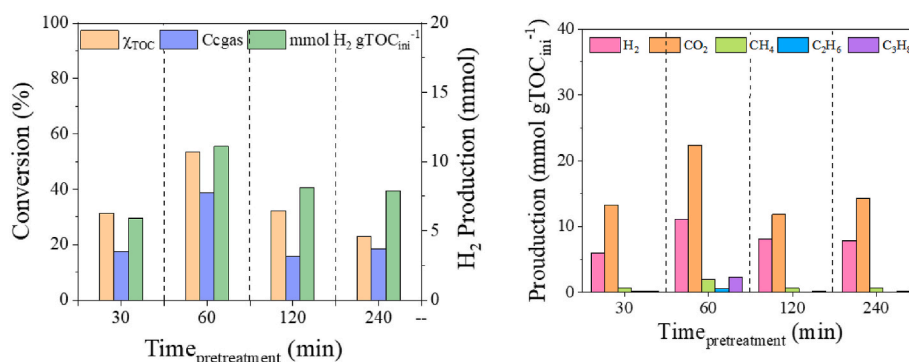


Fig. 6. APR of hydrolysate obtained at different times (pretreatment: 200 °C; APR: TOCini = 1,000 mg/L, 3 % wt. Pt/CB).

when it was increased to 2,000 and 3,000 mg/L. In addition to this, higher Ccgas and H₂ production can be observed also in the experiments performed with the lower initial TOC concentration. This behavior, in agreement to several previously reported works [25,26,33,67], suggests that for higher initial carbon concentration, even though more feedstock is available for reforming, H₂-consuming, HTC, condensation and other secondary reactions are favored, resulting in a lower H₂ and higher alkanes and CO₂ production. This can also be observed from the selectivity to gases shown in Fig. 4, where the CO₂/H₂ ratio decreased for the experiment at initial concentration of 1,000 mg/L. Thus, it has been reported that HTC route results mostly in the generation of CO₂ [68]. Although substantially higher conversion could be expected using a starting concentration lower than 1,000 mg/L [28], previous works on the APR of wastewaters have shown that the lower concentration limit to achieve thermal sustainability of the APR process is around 1 % wt [69]. In addition to H₂, APR of hydrolysate produced a significant amount of alkanes, particularly CH₄, although C₃H₈ was also relevant in the experiments at an initial TOC concentration of 1,000 mg/L.

Although the APR tests reproducibility has been checked and reported in previous works [29], a selected was carried out in triplicate; the results showed a very low dispersion (4–7 %), as showed in Fig. S3 (Supplementary Material).

The biomass pretreatment temperature had a minor influence in the reforming ability of the hydrolysate, as can be observed in the APR results shown in Fig. 5. However, some trend can be observed in Ccgas, which decreased with pretreatment temperature, mainly due to lower generation of CO₂. This may be related to a lower contribution of reactions leading to HTC, since H₂ production remained in similar values regardless the biomass pretreatment temperature. On the contrary, biomass pretreatment time had a more evident influence on the APR results, as shown in Fig. 6, in line with the relevant differences observed for biomass solubilization in the pretreatment. However, organic matter conversion and Ccgas values were low for the hydrolysate obtained in pretreatment for 30 min, in spite of being the conditions leading to

higher solubilization of biomass. In such conditions, less evolved hydrolysis products can be expected to be produced, including extracts and sugars and oligomers from holocellulose fraction [49], which are more difficult to reform. The organic matter conversion and Ccgas obtained for the hydrolysate produced in the pretreatment at 60 min was higher, reaching also a H₂ production ca. 11 mmol per g of initial organic carbon. For higher pretreatment temperatures, a decline in conversion and in H₂ production can be observed. It must be noted that the decline in H₂ production is moderate, whereas a more evident decrease in conversion and CO₂ production was observed, which could be related to a lower presence of organic matter undergoing HTC in the hydrolysate. Longer pretreatment time led to lower conversion and Ccgas, although remarkable selectivity to H₂ was observed in the APR of the hydrolysate produced with a pretreatment temperature of 120 min. In addition to this, a higher presence of compounds more refractory to reforming can be expected in the hydrolysate obtained by pretreatment for 240 min, due to higher intensity of the hydrolysis conditions. In addition, at longer times, compounds more refractory to reforming at 220 °C were observed, such as glycolic acid [70], and at shorter pretreatment times, hydrolysate with a higher acetic acid content is obtained (see supplementary material, Fig. S4) [26,71].

3.3.1. Influence of initial pretreatment pH

The effect of the intensity of hydrolysis conditions during pretreatment can also be seen in Fig. 7, where the APR results for the hydrolysate obtained at different pretreatment starting pH values are shown. Similar conversion values can be observed for the hydrolysate produced at pH values of 1 and 7, however a dramatic decrease in H₂ production is observed for the pH 1 hydrolysate. This behaviour is indicative of the generation of products with low reforming ability during the pretreatment, such as organic acids or sugar and alcohol dehydration products, although these compounds seem to be transformed also by HTC as shown by the high production of CO₂. Despite the low H₂ presence, a relevant production of alkanes is observed, which can be attributed to

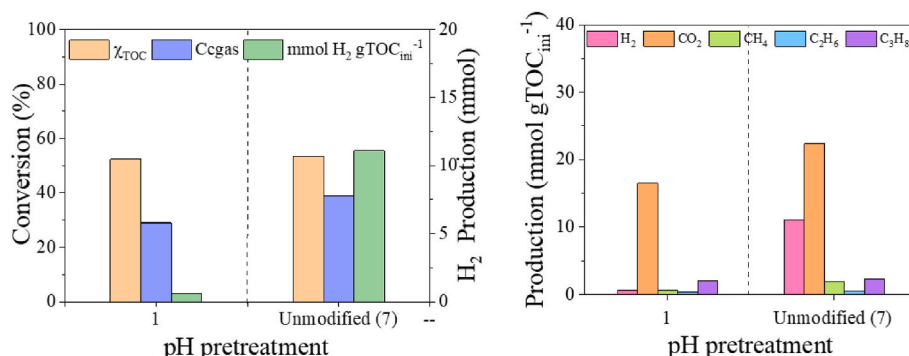


Fig. 7. APR of hydrolysate obtained at different pretreatment pH starting value (pretreatment: 200 °C, 60 min; APR: TOCini = 1,000 mg/L, 3 % wt. Pt/CB).

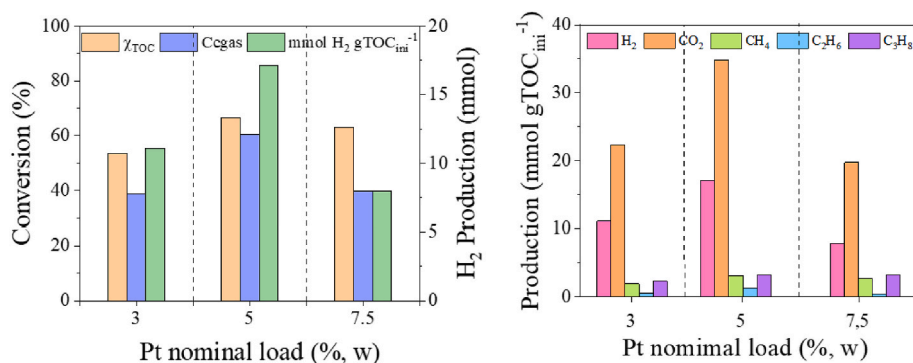


Fig. 8. APR of hydrolysates with catalyst of different metal load (pretreatment: 200 °C, 60 min; APR: TOCini = 1,000 mg/L).

methanation, Fischer-Tropsch reactions, and combination of dehydration and hydrogenation of alcohols produced by the hydrogenation of sugars, but also to reactions involving C–O bond cleavage and hydrogenation [14,72]. Due to the poor results in the APR of the hydrolysate obtained in the pretreatment at pH 1, additional initial TOC values and APR conditions were not studied.

The H₂ production values shown above are somewhat low compared to other case studies where wastewater bearing biomass derived pollutants was treated by APR [19,26,33], showing the refractory nature of the organic compounds solubilized in the hydrothermal pretreatment of lignocellulosic biomass. However, compared to studies on the APR of lignocellulosic biomass in the literature, H₂ production is higher to that found for corn kernel (ca. 9 mmol H₂/gTOCini) and kenaf (ca. 5–13 mmol H₂/gTOCini) biomasses [73,74], but lower to those for switchgrass (ca. 25–45 mmol H₂/gTOCini), miscanthus (ca. 24–28 mmol H₂/gTOCini) and wheat straw (43–56 mmol H₂/gTOCini) biomass [75–77], but it is worthy to note that in these works, the hydrolysis step has been performed at very high temperatures, supercritical extraction or microwave treatment and that the APR was performed at higher temperature up to 250 °C.

3.3.2. Effect of metal concentration in the catalyst

With the aim to increase the reforming of the hydrolysate, the load of catalyst was increased, by increasing the nominal Pt concentration in the catalyst from 3 to 5 and 7.5 % wt. As shown in Fig. 8, the higher availability catalytic sites achieved when Pt concentration in the catalyst was increased from 3 to 5 % wt., resulted in a moderately higher organic matter conversion, and more significantly in a rise of CCgas and H₂ production (by ca. 30 % and above 17 mmol H₂/gTOCini respectively) suggesting an improve of reforming and WGS reactions, although no relevant change in selectivity to H₂ was observed due to high CO₂ generation. However, further increase in Pt load up to 7.5 % wt. resulted in a slightly wider metal particle size distribution and the formation of clearly visible particle aggregates, although the mean size remains similar to that determined for the case of 3 % wt. Pt catalyst (Fig. 1). In consequence, the reforming reaction extension (and therefore the H₂ production) decreases to similar values to those observed for the 3 % wt. Pt catalyst. The TEM images of the different catalysts showed an increase in metal nanoparticle size from 1.9 to ca. 2.8 nm was observed when the Pt content was increased from 3 to 5 and 7.5 % wt., which may be ascribed to Ostwald ripening and has been also observed for the APR of other feedstocks [25].

Fig. S5 shows the thermogravimetric analysis of the catalysts used in the APR reactions. TPD profiles show well defined elbows in the 200–300 °C interval, which can be ascribed to desorption of compounds uptaken by the catalyst in the reaction medium, and beyond 350–400 °C that are related with thermal decomposition of condensed matter deposited on the catalyst [4]. The TPO curves show minor differences respect to the fresh catalyst, indicating low relevance or absence formation of coke structures. Interestingly, the weight loss in TPD assay is

significantly higher for the catalyst with a 3 % wt. Pt load, most probably due to reactions competing with APR and leading to compounds that are deposited, because of lower amount of active sites. This can be confirmed by a delay in the burn-off in the TPO curve, as the metal phase is covered in larger extent by deposited matter thus hampering catalysed oxidation. This effect can also be observed for the 5 % wt. Pt catalyst.

4. Conclusions

Hydrothermal treatment of pruning waste has been used to produce a hydrolysate rich in organic matter suitable for further processing via APR. Within the temperature range studied a higher organic carbon concentration was observed for the treatment at 180 °C, due to hydrolysis of hemicellulose and cellulose and low contribution of recondensation of lignin derivatives. Longer treatment time led to lower dissolution of organic carbon, most probably due to higher extension of condensation reactions. The pretreatment pH affected organic carbon concentration in the hydrolysate, with lower pH values resulting in higher acid-driven hydrolysis and subsequently dissolved carbon concentration.

Hydrogen production by APR of the hydrolysate was influenced by the concentration of organic carbon in the reaction medium, with lower concentration enhancing production. Crossed effect was observed between hydrothermal treatment and APR. Thus, longer hydrothermal pretreatment times and higher temperatures tend to decrease conversion and gas yields in APR due to higher presence of refractory compounds. Increasing the Pt catalyst content enhanced conversion and gas production, although Pt loading above 7.5 % wt. diminished activity. Characterization of the used catalysts showed non-relevant changes in the dispersion of the Pt phase, and some deposition of both light compounds more evolved condensation products.

Declaration of competing interest

The authors declare the following financial interests/personal relationships which may be considered as potential competing interests: Maria Torres reports financial support, equipment, drugs, or supplies, and travel were provided by Government of Spain. Ministry of Science and Innovation. Jessica Justicia reports financial support, equipment, drugs, or supplies, and travel were provided by Government of Spain. Ministry of Science and Innovation. Jose A Baeza reports equipment, drugs, or supplies and travel were provided by Government of Spain. Ministry of Science and Innovation. Luisa Calvo reports financial support, equipment, drugs, or supplies, and travel were provided by Government of Spain. Ministry of Science and Innovation. Francisco Heras reports financial support, equipment, drugs, or supplies, and travel were provided by Government of Spain. Ministry of Science and Innovation. Miguel A Gilarranz reports equipment, drugs, or supplies and travel were provided by Government of Spain. Ministry of Science and Innovation.

Acknowledgements

This work was supported by Spanish Ministry of Science and Innovation [Recovery, Transformation and Resilience Plan, project HYDROCIRCLE, TED2021-130054B-I00] and Community of Madrid (research network BIO3, P2018/EMT- 4344). María Torres thanks support from Spanish Ministry of Science and Innovation through the project HYDROCIRCLE [TED2021-130054B-I00]. Jessica Justicia thanks support from Ministry of Science, Innovation and University through the project WASTEVALOR [PID2019-108445RB-I00].

Appendix A. Supplementary data

Supplementary data to this article can be found online at <https://doi.org/10.1016/j.ijhydene.2024.03.182>.

References

- [1] Huang M, Zhai P. Achieving Paris agreement temperature goals requires carbon neutrality by middle century with far-reaching transitions in the whole society. *Adv Clim Change Res* 2021;12(2):281–6. <https://doi.org/10.1016/j.accre.2021.03.004>.
- [2] Li D, Ma X, Su P, Yang S, Jiang Z, Li Y, Jin Z. Effect of phosphating on NiAl-LDH layered double hydroxide form S-scheme heterojunction for photocatalytic hydrogen evolution. *Mol Catal* 2021;516:111990. <https://doi.org/10.1016/j.mcat.2021.111990>.
- [3] Qureshi F, Yusuf M, Kamyab H, Vo DN, Chelliapan S, Joo S, Vasseghian Y. Latest eco-friendly avenues on hydrogen production towards a circular bioeconomy: currents challenges, innovative insights, and future perspectives. *Renew Sustain Energy Rev* 2022;168:112916. <https://doi.org/10.1016/j.rser.2022.112916>.
- [4] Oliveira AM, Beswick RR, Yan Y. A green hydrogen economy for a renewable energy society. *Curr Opin Chem Eng* 2021;33:100701. <https://doi.org/10.1016/j.coche.2021.100701>.
- [5] European Commission. Communication from the commission to the European Parliament, Europ Council, The Council, The Europ Econom Soci Committee The Committee Region New Circul Econom Act Plan - A Clean More Compet Europe 2020. Retrieved from <https://eur-lex.europa.eu/legal-content/EN/TXT/?uri=CELEX:52020DC0301>.
- [6] Ishaq H, Dinçer İ, Crawford C. A review on hydrogen production and utilization: challenges and opportunities. *Int J Hydrogen Energy* 2022;47(62):26238–64. <https://doi.org/10.1016/j.ijhydene.2021.11.149>.
- [7] Rostrop-Nielsen T. Manufacture of hydrogen. *Catal Today* 2005;106(1–4):293–6. <https://doi.org/10.1016/j.cattod.2005.07.149>.
- [8] Damen K, Van Troost M, Faaij A, Turkenburg W. A comparison of electricity and hydrogen production systems with CO₂ capture and storage. Part A: review and selection of promising conversion and capture technologies. *Prog Energy Combust Sci* 2006;32(2):215–46. <https://doi.org/10.1016/j.pecs.2005.11.005>.
- [9] Boretta A, Banik BK. Advances in hydrogen production from natural gas reforming. *Advan Energy Sustain Res* 2021;2(11). <https://doi.org/10.1002/aesr.202100097>.
- [10] LeRoy RL. Industrial water electrolysis: present and future. *Int J Hydrogen Energy* 1983;8(6):401–17. [https://doi.org/10.1016/0360-3199\(83\)90162-3](https://doi.org/10.1016/0360-3199(83)90162-3).
- [11] Ni M, Leung DY. Energy and exergy analysis of hydrogen production by a proton exchange membrane (PEM) electrolyzer plant. *Energy Convers Manag* 2008;49(10):2748–56. <https://doi.org/10.1016/j.enconman.2008.03.018>.
- [12] Lutz AE, Bradshaw RW, Keller JO, Witmer D. Thermodynamic analysis of hydrogen production by steam reforming. *Int J Hydrogen Energy* 2003;28(2):159–67. [https://doi.org/10.1016/S0360-3199\(02\)00053-8](https://doi.org/10.1016/S0360-3199(02)00053-8).
- [13] Rossi F, Nicolini A. An experimental investigation to improve the hydrogen production by water photoelectrolysis when cyanin-chloride is used as sensitizer. *Appl Energy* 2012;97:763–70. <https://doi.org/10.1016/j.apenergy.2011.11.034>.
- [14] Davda R, Shabaker JW, Huber GW, Cortright RD, Dumesic JA. A review of catalytic issues and process conditions for renewable hydrogen and alkanes by aqueous-phase reforming of oxygenated hydrocarbons over supported metal catalysts. *Appl Catal, B* 2005;56(1–2):171–86. <https://doi.org/10.1016/j.apcatb.2004.04.027>.
- [15] Wei Y, Lei H, Liu Y, Wang L, Zhu L, Zhang X, Yadavalli G, Ahiring BK, Chen S. Renewable hydrogen produced from different renewable feedstock by aqueous-phase reforming process. *J Sustain Bioenergy Syst* 2014;4(2):113–27. <https://doi.org/10.4236/jsbs.2014.42011>.
- [16] Wang Y, Liu B, Guo Q, Sun Y, Zhang S, Qu Y. Stabilized *OH species by K⁺-doped Pt for H₂ generation with ultra-low levels of CO through aqueous-phase reforming of methanol at low temperature. *Appl Catal, B* 2023;338:123011. <https://doi.org/10.1016/j.apcatb.2023.123011>.
- [17] Pipitone G, Zoppi G, Pirone R, Bensaid S. A critical review on catalyst design for aqueous phase reforming. *Int J Hydrogen Energy* 2022;47(1):151–80. <https://doi.org/10.1016/j.ijhydene.2021.09.206>.
- [18] Bhatia L, Garlapati VK, Chandel AK. Scalable technologies for lignocellulosic biomass processing into cellulosic ethanol. *Horizons Bioproc Eng* 2019:73–90. https://doi.org/10.1007/978-3-030-29069-6_5.
- [19] Zoppi G, Pipitone G, Pirone R, Bensaid S. Aqueous phase reforming process for the valorization of wastewater streams: application to different industrial scenarios. *Catal Today* 2022;387:224–36. <https://doi.org/10.1016/j.cattod.2021.06.002>.
- [20] Shahbudin MI, Jacob DM, Ameen M, Aqsha A, Azizan MT, Yusoff MHM, Sher F. Liquid value-added chemicals production from aqueous phase reforming of sorbitol and glycerol over sonosynthesized Ni-based catalyst. *J Environ Chem Eng* 2021;9(4):105766. <https://doi.org/10.1016/j.jece.2021.105766>.
- [21] Alvear M, Aho A, Simakova IL, Grénman H, Salmi T, Murzin DY. Aqueous phase reforming of alcohols over a bimetallic Pt-Pd catalyst in the presence of formic acid. *Chem Eng J* 2020;398–125541. <https://doi.org/10.1016/j.cej.2020.125541>.
- [22] Nozawa T, Mizukoshi Y, Yoshida A, Naito S. Aqueous phase reforming of ethanol and acetic acid over TiO₂ supported Ru catalysts. *Appl Catal, B* 2014;146:221–6. <https://doi.org/10.1016/j.apcatb.2013.06.017>.
- [23] Irmak S, Tiryaki ON. Is it economical and beneficial to produce hydrogen from excess corn kernels? *Fuel* 2020;272:117747. <https://doi.org/10.1016/j.fuel.2020.117747>.
- [24] Kalekar VN, Vaidya PD. Hydrogen production by reforming of sodium alginate in the liquid phase over Pt/C catalyst. *Ind Eng Chem Res* 2021;60(27):9755–63. <https://doi.org/10.1021/acs.iecr.1c01252>.
- [25] Justicia J, Baeza J, Oliveira A, Calvo L, Heras F, Gilarranz MA. Aqueous-phase reforming of water-soluble compounds from pyrolysis bio-oils. *Renew Energy* 2022;199:895–907. <https://doi.org/10.1016/j.renene.2022.09.021>.
- [26] Oliveira AS, Baeza J, Calvo L, Gilarranz MA. Aqueous phase reforming of starch wastewater over Pt and Pt-based bimetallic catalysts for green hydrogen production. *Chem Eng J* 2023;460–141770. <https://doi.org/10.1016/j.cej.2023.141770>.
- [27] Oliveira AS, Baeza JA, Garcia D, Saenz de Miera L, Calvo L, Rodriguez JJ, Gilarranz MA. Effect of basicity in the aqueous phase reforming of brewery wastewater for H₂ production. *Renew Energy* 2020;148:889–96. <https://doi.org/10.1016/j.renene.2019.10.173>.
- [28] Oliveira AS, Baeza JA, Calvo L, Alonso-Morales N, Heras F, Rodriguez JJ, Gilarranz MA. Production of hydrogen from brewery wastewater by aqueous phase reforming with Pt/C catalysts. *Appl Catal, B* 2019;245:367–75. <https://doi.org/10.1016/j.apcatb.2018.12.061>.
- [29] Oliveira AS, Baeza J, Calvo L, Alonso-Morales N, Heras F, Lemus J, Rodriguez JJ, Gilarranz MA. Exploration of the treatment of fish-canning industry effluents by aqueous-phase reforming using Pt/C catalysts. *Environ Sci* 2018;4(12):1979–87. <https://doi.org/10.1039/c8ew00414e>.
- [30] Remón J, García L, Arauzo J. Cheese whey management by catalytic steam reforming and aqueous phase reforming. *Fuel Process Technol* 2016;154:66–81. <https://doi.org/10.1016/j.fuproc.2016.08.012>.
- [31] Saenz de Miera B, Oliveira AS, Baeza JA, Calvo L, Rodriguez JJ, Gilarranz MA. Treatment and valorisation of fruit juice wastewater by aqueous phase reforming: effect of pH, organic load and salinity. *J Clean Prod* 2020;252:119849. <https://doi.org/10.1016/j.jclepro.2019.119849>.
- [32] Lozano P, Simón AI, García L, Ruiz J, Oliva M, Arauzo J. Influence of the Ni-Co/Al-Mg catalyst loading in the continuous aqueous phase reforming of the bio-oil aqueous fraction. *Processes* 2021;9(1):81. <https://doi.org/10.3390/pr9010081>.
- [33] Oliveira AS, Sarrion A, Baeza JA, Díaz E, Calvo L, Mohedano A, Gilarranz MA. Integration of hydrothermal carbonization and aqueous phase reforming for energy recovery from sewage sludge. *Chem Eng J* 2022;442:136301. <https://doi.org/10.1016/j.cej.2022.136301>.
- [34] Zoppi G, Deorsola FA, Galletti C, Rizzo AL, Chiaramonti D, Pirone R, Bensaid S. Aqueous phase reforming of lignin-rich hydrothermal liquefaction by-products: a study on catalyst deactivation. *Catal Today* 2021;365:206–13. <https://doi.org/10.1016/j.cattod.2020.08.013>.
- [35] Oliet M, Rodríguez F, Santos A, Gilarranz MA, García-Ochoa F, Tijero J. Organosolv delignification of eucalyptus globulus: kinetic study of autocatalyzed ethanol pulping. *Ind Eng Chem Res* 1999;39(1):34–9. <https://doi.org/10.1021/ie9905005>.
- [36] Ovejero-Pérez A, Rigual V, Domínguez JC, Alonso M, Oliet M, Rodríguez F. Effect of autohydrolysis and ionosolv treatments on eucalyptus fractionation and recovered lignin properties. *RSC Adv* 2023;13(15):10338–48. <https://doi.org/10.1039/d2ra08013c>.
- [37] Pipitone G, Zoppi G, Bocchini S, Rizzo AM, Chiaramonti D, Pirone R, Bensaid S. Aqueous phase reforming of the residual waters derived from lignin-rich hydrothermal liquefaction: investigation of representative organic compounds and actual biorefinery streams. *Catal Today* 2020;345:237–50. <https://doi.org/10.1016/j.cattod.2019.09.040>.
- [38] Cai J, He Y, Yu X, Banks SW, Yang Y, Zhang X, Yu Y, Liu R, Bridgwater AV. Review of physicochemical properties and analytical characterization of lignocellulosic biomass. *Renewable Sustainable Energy Rev* 2017;76:309–22. <https://doi.org/10.1016/j.rser.2017.03.072>.
- [39] Duman G, Balmuk G, Cay H, Kantarli IC, Yanik J. Comparative evaluation of torrefaction and hydrothermal carbonization: effect on fuel properties and combustion behavior of agricultural wastes. *Energy Fuel* 2020;34(9):11175–85. <https://doi.org/10.1021/acs.energyfuels.0c02255>.
- [40] Libra JA, Ro KS, Kammann C, Funke A, Berge ND, Neubauer Y, Titirici M, Fühner C, Bens O, Kern J, Emmerich K. Hydrothermal Carbonization of biomass residuals: a comparative review of the chemistry, processes and applications of wet and dry pyrolysis. *Biofuels* 2011;2(1):71–106. <https://doi.org/10.4155/bfs.10.81>.
- [41] Urban bioeconomy. From biowastes to biofuels and bio-based chemicals. 2024. <https://madrid.bio3project.es/what-is-bio3/?lang=en>. Last access: Jan.
- [42] Samuelsson R, Burvall J, Jirjis R. Comparison of different methods for the determination of moisture content in biomass. *Biomass Bioenergy* 2006;30(11):929–34. <https://doi.org/10.1016/j.biombioe.2006.06.004>.
- [43] Kumar P, Barrett DM, Delwiche MJ, Stroeve P. Methods for pretreatment of lignocellulosic biomass for efficient hydrolysis and biofuel production. *Ind Eng Chem Res* 2009;48:3713–29. <https://doi.org/10.1021/ie801542g>.

- [44] Suarez E, Tobajas M, Mohedano A, De La Rubia M. Energy recovery from food waste and garden and park waste: anaerobic co-digestion versus hydrothermal treatment and anaerobic co-digestion. *Chemosphere* 2022;297:134223. <https://doi.org/10.1016/j.chemosphere.2022.134223>.
- [45] Rivas S, Santos V, Parajó JC. Effects of hydrothermal processing on miscanthus × giganteus polysaccharides: a kinetic assessment. *Polymers* 2022;14(21):4732. <https://doi.org/10.3390/polym14214732>.
- [46] Lemus J, Bedia J, Calvo L, Simakova IL, Murzin DY, Etzold BJM, Rodriguez JJ, Gilarranz MA. Improved synthesis and hydrothermal stability of Pt/C catalysts based on size-controlled nanoparticles. *Catal Sci Technol* 2016;6(13):5196–206. <https://doi.org/10.1039/c6cy00403b>.
- [47] Joshi AN, Vaidya PD. Hydrogen production by aqueous phase reforming of synthetic sewage using Pt/C catalyst: effect of reaction parameters and pre-treatment strategies. *Waste Biomass Valorization* 2023. <https://doi.org/10.1007/s12649-023-02187-4>.
- [48] Garrote G, Domínguez H, Parajó JC. Hydrothermal processing of lignocellulosic materials. *Eur J Wood Wood Prod* 1999;57(3):191–202. <https://doi.org/10.1007/s001070050039>.
- [49] Santos TM, Alonso MV, Oliet M, Domínguez JC, Rigual V, Rodríguez F. Effect of autohydrolysis on pinus radiata wood for hemicellulose extraction. *Carbohydr Polym* 2018;194:285–93. <https://doi.org/10.1016/j.carbpol.2018.04.010>.
- [50] Deb S, Labafzadeh SR, Liimatainen U, Parviainen A, Hauru LKJ, Azhar S, Lawoko M, Kulomaa T, Kakko T, Fiskari J, Borrega M, Sixta H, Kilpeläinen I, King AWT. Application of mild autohydrolysis to facilitate the dissolution of wood chips in direct-dissolution solvents. *Green Chem* 2016;18(11):3286–94. <https://doi.org/10.1039/c6gc00183a>.
- [51] Zhao H, Gao W, Fatehi P. In-situ polymerization of lignocelluloses of autohydrolysis process with acrylamide. *J Bioresour Bioprod* 2023;8(3):235–45. <https://doi.org/10.1016/j.jobab.2023.01.004>.
- [52] Carvalho DM, Colodette JL. Comparative study of acid hydrolysis of lignin and polysaccharides in biomasses. *Bioresources* 2017;12(4):6907–23. <https://doi.org/10.15376/biores.12.4.6907-6923>.
- [53] Leschinsky M, Zuckerstätter G, Weber HK, Patt R, Sixta H. Effect of autohydrolysis of eucalyptus globulus wood on lignin structure. Part 1: comparison of different lignin fractions formed during water prehydrolysis. *Holzforschung* 2008;62(6): 645–52. <https://doi.org/10.1515/hf.2008.117>.
- [54] Ischia G, Fiori L. Hydrothermal carbonization of organic waste and biomass: a review on process, reactor, and plant modeling. *Waste Biomass Valorization* 2020; 12(6):2797–824. <https://doi.org/10.1007/s12649-020-01255-3>.
- [55] Ipiates P, Mohedano A, Diaz E, De La Rubia M. Energy recovery from garden and park waste by hydrothermal carbonisation and anaerobic digestion. *Waste Manage (Tucson, Ariz)* 2022;140:100–9. <https://doi.org/10.1016/j.wasman.2022.01.003>.
- [56] Lucian M, Volpe M, Fiori L. Hydrothermal carbonization kinetics of lignocellulosic agro-wastes: experimental data and modeling. *Energies* 2019;12(3):516. <https://doi.org/10.3390/en12030516>.
- [57] Zhao H, Gao W, Fatehi P. Interaction of lignin and hemicelluloses in hydrolysate and with stainless steel surface. *Wood Sci Technol* 2022;56:793–812. <https://doi.org/10.1007/s00226-022-01376-z>.
- [58] Loaiza JM, López F, García MT, Fernández OR, Díaz MJM, García JCF. Selecting the pre-hydrolysis conditions for eucalyptus wood in a fractional exploitation biorefining scheme. *J Wood Chem Technol* 2016;36(3):211–23. <https://doi.org/10.1080/02773813.2015.1112402>.
- [59] Bhatto AW, Qureshi K, Harijan K, Abro R, Abbas T, Bazmi AA, Karim S, Yu G. Insight into progress in pre-treatment of lignocellulosic biomass. *Energy* 2017;122: 724–45. <https://doi.org/10.1016/j.energy.2017.01.005>.
- [60] Rivas S, Santos V, Parajó JC. Effects of hydrothermal processing on miscanthus × giganteus polysaccharides: a kinetic assessment. *Polymers* 2022;14(21):4732. <https://doi.org/10.3390/polym14214732>.
- [61] Bielen A, Verhaart M, Oost J, Kengen S. Biohydrogen production by the thermophilic bacterium *Caldicellulosiruptor saccharolyticus*: current status and perspectives. *Life* 2013;3(1):52–85. <https://doi.org/10.3390/life3010052>.
- [62] Evcil T, Simsir H, Ucar S, Tekin K, Karagöz S. Hydrothermal carbonization of lignocellulosic biomass and effects of combined Lewis and Brønsted acid catalysts. *Fuel* 2020;279:118458. <https://doi.org/10.1016/j.fuel.2020.118458>.
- [63] Yang Z, Cao L, Li Y, Zhang M, Zeng F, Yao S. Effect of pH on hemicellulose extraction and physicochemical characteristics of solids during hydrothermal pretreatment of eucalyptus. *Bioresources* 2020;15(3):6627–35. <https://doi.org/10.15376/biores.15.3.6627-6635>.
- [64] López F, García MT, Ferial M, García JCF, de Diego C, Zamudio A, Díaz MJM. Optimization of furfural production by acid hydrolysis of eucalyptus globulus in two stages. *Chem Eng J* 2017;240:195–201. <https://doi.org/10.1016/j.cej.2013.11.073>.
- [65] Gellerstedt G, Li J. Improved lignin properties and reactivity by modifications in the autohydrolysis process of aspen wood. *Ind Crops Prod* 2008;27(2):175–81. <https://doi.org/10.1016/j.indcrop.2007.07.022>.
- [66] Lu F, Yazdi S, Frazier CE. Catalytic acidolysis: impact on in situ pine-lignin repolymerization. *ACS Sustainable Chem Eng* 2023;11(29):10709–16. <https://doi.org/10.1021/acssuschemeng.3c01341>.
- [67] Luo N, Fu X, Cao F, Xiao T, Edwards PP. Glycerol aqueous phase reforming for hydrogen generation over Pt catalyst – effect of catalyst composition and reaction Conditions. *Fuel* 2008;87:3483–9. <https://doi.org/10.1016/j.fuel.2008.06.021>.
- [68] Reza MT, Andert J, Wirth B, Busch D, Pielert J, Lynam JG, Mumme J. Hydrothermal carbonization of biomass for energy and crop production. *Appl Bioenergy* 2014;1(1):11–29. <https://doi.org/10.2478/apbi-2014-0001>.
- [69] Heras F, Oliveira A, Baeza J, Calvo L, Ferró VR, Gilarranz MA. Toward sustainability of the aqueous phase reforming of wastewater: heat recovery and integration. *Appl Sci* 2022;12(20):10424. <https://doi.org/10.3390/app122010424>.
- [70] Pipitone G, Zoppi G, Bocchini S, Rizzo AM, Chiaramonti D, Pirone R, Bensaid S. Aqueous phase reforming of the residual waters derived from lignin-rich hydrothermal liquefaction: investigation of representative organic compounds and actual biorefinery streams. *Catal Today* 2020;345:237–50. <https://doi.org/10.1016/j.cattod.2019.09.040>.
- [71] Amin FR, Khalid H, Zhang H, Rahman S, Zhang R, Liu G, Chen C. Pretreatment methods of lignocellulosic biomass for anaerobic digestion. *Amb Express* 2017; 7–72. <https://doi.org/10.1186/s13568-017-0375-4>.
- [72] Cortright RD, Davda RR, Dumesic JA. Hydrogen from catalytic reforming of biomass-derived hydrocarbons in liquid water. *Nature* 2020;418(6901):964–7. <https://doi.org/10.1038/nature01009>.
- [73] Tiriyaki ON, Irmak S, Ramchandran D, Subbiah J, Morton MD. Utilization of excess corn kernels for hydrogen gas biofuel production. *Int J Hydrogen Energy* 2019;44 (57):29956–63. <https://doi.org/10.1016/j.ijhydene.2019.09.212>.
- [74] Irmak S, Öztürk İ. Hydrogen rich gas production by thermocatalytic decomposition of kenaf biomass. *Int J Hydrogen Energy* 2010;35(11):5312–7. <https://doi.org/10.1016/j.ijhydene.2010.03.081>.
- [75] Irmak S, Meryemoglu B, Sandip A, Subbiah J, Mitchell RB, Sarath G. Microwave pretreatment effects on switchgrass and miscanthus solubilization in subcritical water and hydrolysate utilization for hydrogen production. *Biomass Bioenergy* 2018;108:48–54. <https://doi.org/10.1016/j.biombioe.2017.10.039>.
- [76] Meryemoglu B, Kaya B, Irmak S, Hesenov A, Erbatur O. Comparison of batch aqueous-phase reforming of glycerol and lignocellulosic biomass hydrolysate. *Fuel* 2012;97:241–4. <https://doi.org/10.1016/j.fuel.2012.02.011>.
- [77] Kaya B, Irmak S, Hasanoglu A, Erbatur O. Evaluation of various carbon materials supported Pt catalysts for aqueous-phase reforming of lignocellulosic biomass hydrolysate. *Int J Hydrogen Energy* 2014;39(19):10135–40. <https://doi.org/10.1016/j.ijhydene.2014.04.180>.